JODR
Volume 10, Issue 3, 2023

Assessment of Some Mechanical Properties of CNC Laser Treated Ti13Zr13Nb Alloy

[1]Azhar Imran Alawadi, MSc and [2]Aseel Mohammed Al-Khafaji, PhD
[1] Department of Prosthodontic, College of Dentistry, University of Thi Qar, Thi Qar, Iraq.
[2] Department of Prosthodontic, College of Dentistry, University of Baghdad, Baghdad, Iraq.

Corresponding author: Azhar Imran Alawadi
E. Mail: azher-o-alawady@utq.edu.iq

Received 20 January 2023.
Accepted for publication on July 22, 2023.
Published November 28, 2023.
Doi: https://doi.org/10.58827/845950rilsoc

Abstract

Background Alloys with the addition of zirconium and niobium eliminate the adverse effects of aluminum and vanadium on the nervous system, the possibility of metallosis and the initiation of diseases (including cancers or Alzheimer›s disease). In addition, they have better corrosion resistance, and a Young›s modulus value similar to longitudinal bone tissue. Therefore, only choosing appropriate materials does not guarantee proper functioning of the implants, the surfaces of the implants also have to be suitable to meet the requirements. The laser surface hardening process modifies the surface properties by imparting microstructural changes, whereas surface remelting induces changes in the surface topography, roughness, wettability and wear and corrosion resistance, influencing the biocompatibility of the surface. Such changes are brought in essentially because of the characteristic melting, evaporation and rapid solidification during laser surface remelting processes. **Objectives** This study was aimed at evaluating the electrochemical corrosion of commercial pure Titanium disks (CP Ti) and the Ti13Zr13Nb (Alloy) with a zigzag pattern of laser surface treatment. **Materials and Methods** a total of 40 discs of Cp Ti & 40 of Ti13Zr13Nb were fabricated. The surfaces of the test groups were treated with unique zigzag patterns using CNC Laser treatment on the texturing surfaces, the samples then are analyzed by using XRD, microhardness and electrochemical corrosion tests. **Results** The study revealed a proper increase in the surface hardness and corrosion resistance without crack formation or a dramatic change of the core substance of the CP Ti and Alloy disks. **Conclusion** The CNC laser is considered an effective and suitable method for surface texturing of CP Ti and Alloy for dental implantology.

Keywords: Commercial pure Titanium; Ti13Zr13Nb alloy; CNC Laser; laser surface texturing; dental implant and corrosion.

Introduction

Titanium and titanium alloys have been used widely for several decades as the materials of choice for dental implants because of their biocompatibility, good mechanical properties, corrosion resistance, no cell toxicity and weaker inflammatory response in peri-implant tissues. The usage of Ti and its alloys as dental implants may be correlated with some disadvantages despite the good evidence of its usage like the elastic moduli difference between Titanium implant and the surrounding bone, which led to stress in the bone-implant interface and peri-implant bone loss (McSarot et al, 2010). The dental implant surface modification, specifically the topographical, is considered as an effective method for improving the bioactivity of dental implants (Mandracci, 2019). Several studies showed that implant surface modification by the laser technique can reduce dental implant contamination with implant torque removal increasing after their implantation in rabbit tibia and femur (Brånemark et al, 2011; Azzawi et al, 2017; Al Khafaji et al, 2020). The laser surface modification techniques could offer better osseointegration due to the formation of surface microstructures with significant hardness enhancement, corrosion resistance, standard roughness, a high degree of purity and an increase of the oxide layer (Hallgren et al, 2003). Berezani et al. Stated that the oxide layer increases more than doubles after implant surface laser treatment (Berezani et al, 2003). Ti13Zr13Nb is a high-strength, low modulus and biocompatible alloy. Implants of this alloy would have a modulus of elasticity closer to that of bone than other typically-used metal alloys and do not include any elements which have been shown or suggested as having short-term potential adverse effects (Henriques et al, 2005). Ti13Zr13Nb is a near β alloy formulated at the beginning of the 1990s to be used in orthopaedic applications due to its low Young's modulus (40–80 GPa) and its non-toxic composition. It presents tensile values of approximately 1,300 MPa and a superior corrosion resistance when compared to Ti–6Al–4V and Ti–6Al–7Nb alloys (Henriques et al., 2010). The first-generation orthopaedic α+β Titanium alloys such as Ti–6Al–4V ELI (extra low interstitial), Ti–6Al–7Nb and Ti–5Al–2.5Fe are already in use. In recent years, second-generation low-modulus near β and type Titanium alloys have been developed for orthopaedic applications to avoid the "stress shielding" effect caused by the modulus mismatch between the implant and the bone (Ni et al, 2009). The Ti–13Nb–13Zr has Niobium as a beta-phase stabilizer. The other alloying element, Zirconium, is isomorphous with both the alpha and beta phases of Titanium. A combination of these two alloying elements has made it possible to develop a structure that is a "near" beta phase supposedly possessing a superior corrosion resistance over the alpha–beta phase alloys, with enough alpha phase present in the final structure to provide the necessary mechanical strength. It has been proposed that Ti13Nb13Zr alloy is more favourable for orthopaedic implants than Ti6Al4V alloy because of its superior corrosion resistance and biocompatibility. Reasons for this superiority have included the fact that less metal ion release is likely to occur during spontaneous passivation of Ti–13Nb–13Zr alloy because the corrosion products of the minor alloying elements, Niobium and Zirconium, are less soluble than those of aluminium and vanadium. Also, that the passive oxide layer on the surface of the alloy is more inert consisting of a dense rutile structure providing greater protection to the underlying alloy. Due to the complete dissolution of the alloy elements in the Titanium matrix, a good combination of microstructure, mechanical properties and densification could be reached (Steven et al, 2001). Corrosion causes a deterioration of metal surfaces and alloys causing undesirable consequences in terms of replacement, repair, product losses, and safety. For this reason, it is very important to prevent corrosion. Suitable modifications can be made to control the corrosion of metal (Rawaa et al, 2019). Hence, this study aimed to evaluate the corrosion of commercial pure Titanium disks (CP

Ti) and the Ti 13Nb 13 Zr (Alloy) with a zigzag pattern of laser surface structuring with zig-zag lines is the favourable surface treatment of dental implants

Material and Methods

Sample grouping

The CP Ti and Alloy disks were divided into four groups, as follows:

•(Ti) CP Ti control group, without any surface treatment or structuring.
•(TiL) CP Ti with laser surface structuring.
•(TZN) Alloy control group, without any surface treatment or structuring.
•(TZN L) Alloy with laser surface structuring.

Samples preparation

Circular disks, 9 mm diameter and 2 mm thickness of commercial pure Titanium disks (CP Ti) and the Ti 13Nb 13 Zr (Alloy) were cut with a wire cut machine (Knuth Smart DEM-Germany). Then, these disks were polished to a mirror-smooth uniform appearance via rotation machine with sandpapers proceeded from 500 to 2400 grit. For removing contamination, the samples were placed in the ultrasonic cleaning device for 15 minutes with ethanol, and then for 10 minutes with distilled water, respectively. Finally, the samples were dried at room temperature for 15 minutes (Duarte et al, 2009).

Pilot study

Laser surface structuring

Five scanning speeds were tested, 2000, 1200, 500, 300 and 150 mm/sec. Speeds 2000, 1200 and 500 mm/sec. Resulted in creating scattered dots that didn't reveal the pattern required. Speed of 150 mm/sec. made pattern lines overlap and the surface turn blackish grey, which may strongly suggest scorching the surface. The speed of 300 mm/sec. was selected for it created the distinct pattern required without signs of burning the surface nor scattered dots. Three designs were tested before settling for this one. The other ones had right and sharp angles in the zig-zag lines instead of the obtuse ones used in this study. But the other designs were eliminated due to increased wettability angles (reduced surface wettability) since most studies have found that hydrophilic surfaces tend to enhance the early stages of cell adhesion, proliferation, differentiation and bone mineralization compared to hydrophobic surfaces (Al Khafaji et al, 2021). The laser system performed the desired profile on the CP Ti and Alloy disk surfaces. The surfaces of the CP Ti and Alloy were structured under a normal atmosphere by using a pulse mode CNC fibre laser machine (Al Khafaji et al, 2020) (Raycus 50 Watts-China) with laser power 30-Watts, wavelength 1064 nm, Frequency of 200 pulses per second and scanning speed up to 300 mm/sec. Corel Draw software (version XII) was used for drawing the zig-zag design shapes. The samples-laser source disk distance was 22 cm. When the system was triggered, the laser beam started shooting at the sample with a continuous series of laser pulses in an ablation process to form the zig-zag lines design. The lines were made 416.38 µm with 116.1 µm spaces in between the lines. The zig-zag lines were created with an angle of 134.88º. Scanning electron microscope (SEM) images of the samples are shown in Figure (1).

Phase analysis by the X-ray diffraction test

The X-ray diffraction pattern for the control and the laser structure specimens for the 3 different designs on CP Ti groups are shown in Figure (2). The X-ray diffraction pattern for the control and the laser structure specimens for the 3 different designs on Alloy groups are shown in Figure (3). One disk was examined for each group. Laser structuring did not give rise to noteworthy interchanges in the phases of the Ti as seen in the XRD pattern; which is of which is of high importance to ensure biocompatibility after laser irradiation (Al Khafaji et al, 2021). A new peak of TiO2 was observed beside the Ti after laser structuring which could probably be due to the titanium-air interaction during the surface structuring.

The main study

Micro hardness test

Digital Vickers micro-hardness tester was used to record the micro-hardness of the control and laser-treated disks of the CP Ti and the Alloy according to (Al Khafaji et al, 2021), for 15 seconds 500g load was applied to the surface of the disk by using Vickers indenter that joins optical microscopy shown in figure (4). An average of 3 different readings was measured from the ten specimens of each one of the groups.

Electrochemical corrosion

Samples were used for the electrochemical tests. All samples were connected to a copper wire and then mounted in epoxy resin with an exposed area of a 7 mm. diameter & and an area of 0.385 cm2 as the working electrode, as shown in figure (5). Before the electrochemical test, the mounted sample was carefully degreased with acetone and ethanol and rinsed with distilled water, then finally dried in a stream of warm air. The open circuit potential (OCP) and potentiodynamic polarization curves for sample measurements carried out according to the defined ASTM standards (ASTM 2009; 2015; 2017). Soaked in electrolytes such as simulated body fluid (SBF) (Safi, 2019). A Potentiostat, as shown in figure (6), Electrochemical system provided by three-electrode cell system with a saturated Calomel electrode (SCE) as the reference electrode, a platinum electrode (15 x 15 mm2) as the counter-electrode and the sample mounted in epoxy resin as the working electrode was used in this study. The scan rate was 1Mv/sec. for 30 minutes for each sample. All experiments were carried out at a temperature of 37°C controlled by a thermostat (Li et al, 2011) these tests done in the Ministry of Science and Technology-Baghdad- Iraq.

Statistical Methods

All obtained data were analyzed using the one-way Analysis of Variance (ANOVA) and t-test in the GraphPad Prism (version 6.0.1) Software. Differences were considered significant at P>0.05. Values were represented as Mean >Standard Error (M > SE).

Results

Micro hardness test

The test was conducted by applying a load of 5 to 500 gm for a 15 sec. period. Images of the resulting penetration are shown in figure (4). Descriptive statistics of microhardness measured in Kg/mm2 of all groups shown in table (1), demonstrated that the highest average surface hardness was in the TNZ L group while the lowest average was in the Ti group as shown in figure (7). Normality and Lognormality Tests of surface Microhardness (Test for normal distribution Shapiro-Wilk test) shown in table (2) revealed that the P value for all groups is higher than 0.05 (non-significant), which means that data were normally distributed among the groups & and one way ANOVA is applicable.One way ANOVA test demonstrated a highly significance difference in the microhardness among the four groups, P<0.0001 at three degrees of freedoms as shown in table (3). Tukey›s multiple comparisons test of microhardness Multiple comparison shown in table (4) revealed highly significant difference between contact angles between all groups except Ti L vs. TNZ.

Electrochemical corrosion test:

The corrosion tests measuring techniques were involved, Tafel and cyclic polarization; besides open circuit potential. Potentiodynamic polarization test in SBF at 37°C, carried out to evaluate the bio-degradation behavior of Ti, Ti L, TNZ & TNZ L groups. The corrosion rate was calculated according to the formula:

Corrosion Rate (mmpy) = 0.00327 Icorr (EW)/d
Where:
EW: equivalent weight
D: density

Descriptive statistics of electrochemical corrosion for all groups shown in table (5), demonstrated that the highest average corrosion rate was in Ti group while the lowest average was in TNZ

group as shown in figure (8). Normality and Lognormality Tests of corrosion rate (Test for normal distribution Shapiro-Wilk test) shown in table (6) revealed that the P value for Ti & Ti L groups is higher than 0.05 (non-significant), while the P value for the TNZ & TNZ L groups is lower than 0.05 (significant & highly significant respectively) which means that data were not normally distributed among the groups & Kruskal-Wallis testing was applicable. Kruskal–Wallis one-way analysis of variance demonstrated a highly significance difference in the corrosion rate among the four groups, P<0.0001 (highly significant) as shown in table (7) and Dunn's test is applicable. Dunn›s multiple comparisons test of Surface Roughness of among the tested groups revealed that the differences in surface roughness of Ti vs. Ti L, Ti vs. TNZ L & TNZ vs. TNZ L were highly significant, while between Ti vs. TNZ, Ti L vs. TNZ & Ti L vs. TNZ L groups are non-significant, as shown in table (8).

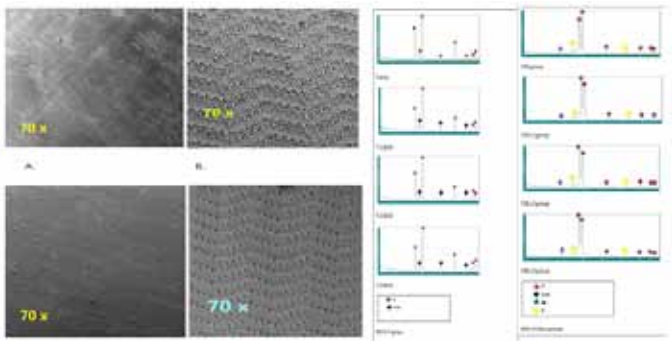

Figure (1): SEM images of the samples A. where sample from Ti group, B. sample from Ti L group C. sample from TZN group & D. sample from TZN L group.
Figure (2): 2 XRD patterns of Ti groups.
Figure (3): XRD patterns of Alloy groups

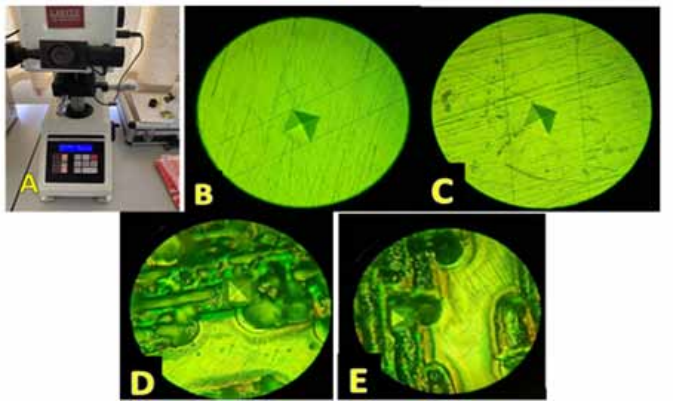

Figure (4): A. Microhardness test machine. B, C, D, E indentation marks on Ti, TNZ, Ti L & TNZ L respectively.

Figure (5): A cylindrical sample mounted by epoxy resin and connected with copper wire.

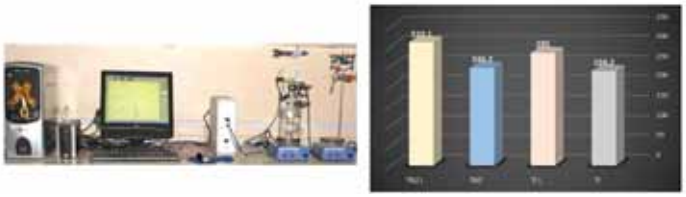

Figure (6): Wenking-M lab Potentiostat.
Figure (7): Mean Microhardness in Kgmm2 for tested group.

Table (1): micro hardness test Descriptive statistic for tested groups.

	Ti	Ti L	TNZ	TNZ L
Number of values	10	10	10	10
Minimum	200.1	249.5	222.8	251.8
Maximum	284.8	301.5	265.8	359.5
Range	84.7	52	43	107.7
Mean	238.2	285	246.2	310.1
Std. Deviation	18.52	12.63	12.22	26.01
Lower 95% CI of mean	231.3	280.3	241.7	300.4
Upper 95% CI of mean	245.1	289.7	250.8	319.8

Table (2): Normality and Lognormality Tests of Microhardness (Test for normal distribution Shapiro-Wilk test).

	Ti	Ti L	TNZ	TNZ L
W	0.9838	0.9392	0.9552	0.9404
P value	0.9149	0.0567	0.2331	0.0931
Passed normality test (alpha=0.05)?	Yes	Yes	Yes	Yes
P value summary	ns	ns	ns	ns

Table (3): Ordinary one-way ANOVA of Microhardness.

ANOVA table	SS	DF	MS	P value
Treatment (between columns)	102168	3	34056	P<0.0001
Residual (within columns)	38525	36	332.1	
Total	140693	39		

Table (4): Ordinary one-way ANOVA of Microhardness Multiple comparison.

Tukey's multiple comparisons test	Mean Diff.	Summary	Adjusted P Value
Ti vs. Ti L	-46.76	****	<0.0001
Ti vs. TNZ	-8.003	ns	0.3279
Ti vs. TNZ L	-71.85	****	<0.0001
Ti L vs. TNZ	38.76	****	<0.0001
Ti L vs. TNZ L	-25.09	****	<0.0001
TNZ vs. TNZ L	-63.85	****	<0.0001

Table (5): Descriptive statistic for Electrochemical corrosion for tested groups.

	Ti	Ti L	TiNZ	TiNZ L
Number of values	10	10	10	10
Minimum	0.01103	0.002176	0.003044	0.000116
Maximum	0.01193	0.002504	0.004874	0.000215
Range	0.0009	0.000328	0.00183	9.90E-05
Mean	0.01144	0.002317	0.003686	0.000189
Std. Deviation	0.00029	0.000109	0.000682	2.65E-05
Lower 95% CI of mean	0.01123	0.002239	0.003198	0.00017
Upper 95% CI of mean	0.01165	0.002395	0.004173	0.000208

Table (6): Normality and Lognormality Tests of Electrochemical Corrosion.

	Ti	Ti L	TiNZ	TiNZ L
W	0.8764	0.8791	0.7979	0.6039
P value	0.1186	0.1274	0.0137	<0.0001
Passed normality test (alpha=0.05)?	Yes	Yes	No	No
P value summary	ns	ns	*	****

Table (7): Kruskal-Wallis test of Electrochemical Corrosion.

P value	<0.0001
P value summary	****
Do the medians vary significant (P < 0.05)?	Yes
Number of groups	4
Kruskal-Wallis statistic	36.59

Table 8: Kruskal-Wallis test of Electrochemical Corrosion by Dunn›s multiple comparisons test.

Dunn's multiple comparisons test	Mean rank diff.	Summary	Adjusted P Value
Ti vs. Ti L	20	***	0.0008
Ti vs. TNZ	10	ns	0.3346
Ti vs. TNZ L	30	****	<0.0001
Ti L vs. TNZ	-10	ns	0.3346
Ti L vs. TNZ L	10	ns	0.3346
TNZ vs. TNZ L	20	***	0.0008

Discussion

A novel implant material the Ti13Nb13Zr alloy seems to be the best choice compared to the widely used commercial alloys, as it possesses Young's modulus approaching that of a bone, and it contains no harmful elements such as Al or V, promising to minimize stress shielding phenomenon and enhancing the longevity of dental implants. Along the use of novel laser surface structuring patterns designed to gain the benefits of both lines-based and dots-based designs from previous studies. This study was aimed to evaluate an important aspect of dental implants: surface hardness and electro-chemical corrosion and how are those characteristics affected with laser surface treatment. Tests results revealed that Ti Group showed lower surface microhardness and Electrochemical corrosion resistance than all the other groups. To obtain the proper prospective; commercially pure Titanium is proven to be very successful in dental implants (Chen et al, 2020), these results can only give high praise to the other groups. TNZ group showed higher surface microhardness and electromechanical corrosion resistance than Ti group, which support the hypothesis of this study that Ti–13Nb–13Zr might be a preferable substrate of dental implants. TiL group showed higher surface microhardness and electromechanical corrosion resistance than both Ti group and TNZ group, which support the hypothesis of this study that CNC laser surface modification might be a preferable surface structuring technique of dental implants. TNZ L group showed higher surface microhardness and electromechanical corrosion resistance than Ti group, TNZ and TNZ groups, which support both hypothesis of this study that Ti–13Nb–13Zr might be a preferable substrate of dental implants, & that CNC laser surface modification might be a preferable surface structuring technique of dental implants. Which coincide with the previous studies that laser surface treatment alloys improve surface qualities relevant to dental implant applications. Which could be attributed to laser remelting (LRM), which involves laser irradiation to improve the surface quality. The remelting of material surfaces using lasers can remove any pores, bead traces, unmelted powder, and spatter from the surface of the deposited layers. Unlike other postprocessing treatments, the areas subjected to laser irradiation are cooled rapidly to obtain a fine microstructure. LRM technology is used on deposited surfaces, and many studies have been conducted for improving the mechanical properties of the surface (John et al, 2020). Yasa and Kruth reported that using selective laser melting showed increased density and improved porosity when subjected to LRM (Seung et al, 2021). Further, Yu et al. employed LRM to improve the porosity and roughness of a treated surfaces (Yu et al, 2020). Studies have also improved the quality and mechanical properties of the surface by changing the process parameters of LRM (Yasa et al, 2011; Wei et al, 2019; Kim et al, 2020 & Aboulkhair et al, 2014).

Conclusions

Laser surface modification of Cp Ti and Ti alloys has pronounced positive effect on enhancement of desirable qualities for the field of dental implants. This study showed that the Ti13Zr13Nb alloy already have much of the mechanical advantages in the field of dental implants over Cp Ti, and can better accept laser surface structuring leading to intensified surface Ti oxide protective layer. Additionally, the adoption of zigzag lines pattern can combine many benefits of previously used patterns of dots or straight lines. In the light of this study, the usage of Ti13Zr13Nb alloy and CNC laser surface modification might resolve some of the problems that were found in other Titanium alloys and might further enhance osseointegration and better serve dental implant purposes.

References

Aboulkhair NT, Everitt NM, Ashcroft I, Tuck C. Reducing porosity in AlSi10Mg parts processed by selective laser melting. Add Manuf 2014; 1:77e86. https://doi.org/10.1016/ j. addma.2014.08.001

Ahmed Al Gabban, Raghdaa K. Jassim, Luma M. Ibrahim: Evaluation of Cytotoxicity and Biocompatibility of Ti2AlC in Rabbits. Journal of Baghdad College of Dentistry
2021, Volume 33, Issue 4, Pages 20-24.

Al-Khafaji, A.M. Laser Surface Structuring and Coating of Titanium Implant with High Performance Poly Ether Ketone Ketone Polymer (In vitro - In vivo) Study. A PhD, College of Dentistry, University of Baghdad, 2020.

Al-Khafaji, A.M.; Hamad, T.I. Assessment of Surface Roughness and Surface Wettability of Laser Structuring Commercial Pure Titanium. J Research Med and Dent Sci 2020, 8(1), 81-85.

Aseel Mohammed Al-Khafaji, Thekra Ismael Hamad: Surface Analysis of the PEKK Coating on the CP Ti Implant Using Laser Technique. International Medical Journal Vol. 28, Supplement No. 1, pp. 29 - 32, June 2021.

Azzawi, Z.G. Osseointegration evaluation of laser-deposited titanium dioxide nanoparticles on commercially pure titanium dental implants. Master thesis, College of Dentistry, University of Baghdad, 2017.

Bereznai, M.; Pelsoczi, I.; Toth, Z.; Turzo, K.; Radnai, M.; Bor, Z.; Fazekas, A. Surface modifications induced by ns and sub-ps excimer laser pulses on titanium implant material. Biomater 2003, 24 (23), 4197-203. https://10.1016/s0142-9612(03)00318-1

Brånemark R, Emanuelsson L, Palmquist A, Thomsen P. Bone response to laser-induced micro- and nano-size titanium surface features. Nanomedicine. 2011 Apr;7(2):220-7.https://doi: 10.1016/j.nano.2010.10.006

CHEN, K., XIE, X., TANG, H., SUN, H., QIN, L., ZHENG, Y., GU, X. & FAN, Y. 2020. In vitro and in vivo degradation behavior of Mg–2Sr–Ca and Mg–2Sr–Zn alloys. Bioactive materials, 5, 275-285.

Duarte, L.T.; Biaggio, S.R.; Rocha Filho, R.C..; Bocchi, N. 2012. Modification of the titanium oxide morphology and composition by a combined chemical-electrochemical treatment on cp Ti. Mat. Res. 15 (1) • Feb 2012 • https://doi.org/10.1590/S1516-14392012005000002

Hallgren C, Reimers H, Chakarov D, Gold J, Wennerberg A. An in vivo study of bone response to implants topographically modified by laser micromachining. Biomaterials. 2003 Feb;24(5):701-10. https://doi: 10.1016/s0142-9612(02)00266-1.

Henriques, V.A.R.; Galvani, E.T.; Petroni, S.L.G.; Paula, M.S.M.; Lemos, T.G. Production of Ti–13Nb–13Zr alloy for surgical implants by powder metallurgy. J Mater Sci 2010, 45 (21),5844–5850

Henriques; V.A.R.; Cairo, C.A.A; Silva, C.R.M. Bressiani, J.C., MICROSTRUCTURAL EVOLUTION OF Ti13Zr13Nb ALLOY DURING SINTERING. Materials Science Forum Vols. 498-499 (2005) pp 40-48.

Safi IN, Hussein BMA, Al Shammari AM, Tawfiq TA. Implementation and characterization of coating pure titanium dental implant with sintered β-TCP by using Nd:YAG laser. Saudi Dent J. 2019 Apr;31(2):242-250. https://doi: 10.1016/j.sdentj.2018.12.004

Ihab Nabeel Safi: Physiological Dental Implant Prepared by Stem Cells with β-TCP Coated Titanium and Zirconia Implants. A PhD, College of Dentistry, University of Baghdad, 2019.

John W. Nicholson: Titanium Alloys for Dental Implants: A Review. Dental Materials Unit, Bart's and the London Institute of Dentistry, Queen Mary University of London, 15 June 2020 Prosthesis and Prosthetic Materials.

Kim TH, Baek GY, Jeon JB, Lee KY, Shim DS, Lee W. Effect of laser rescanning on microstructure and mechanical properties of direct energy deposited AISI 316L stainless steel. Surf Coating Technol 2021; 405:126540. https://doi.org/10.1016/j.surfcoat.2020.126540.

LI, Y. & HODGSON, P. D. 2011. The effects of calcium and yttrium additions on the microstructure, mechanical properties and biocompatibility of biodegradable magnesium alloys. Journal of materials science, 46, 365-371.

Mandracci, P.; Mussano, F.; Rivolo, P.; Carossa, S. Surface Treatments and Functional Coatings for Biocompatibility Improvement and Bacterial Adhesion Reduction in Dental Implantology. Coatings 2016, 6(1), 7-29.

Sarot JR, Contar CM, Cruz AC, de Souza Magini R. Evaluation of the stress distribution in CFR-PEEK dental implants by the three-dimensional finite element method. J Mater Sci Mater Med. 2010 Jul;21(7):2079-85. https://doi: 10.1007/s10856-010-4084-7.

Ni, Y.X.; Feng, B.; Wang, J.; Lu, X.; Qu, S.; Weng, J. Decyl bis phosphonate–protein surface modification of Ti–6Al–4V via a layer-by-layer technique. J Mater Sci, 2009, 44(15), 4031-4039.

Nune KC, Misra RD, Li SJ, Hao YL, Yang R. Osteoblast cellular activity on low elastic modulus Ti-24Nb-4Zr-8Sn alloy. Dent Mater. 2017 Feb;33(2):152-165. https://doi: 10.1016/j.dental.2016.11.005

Oldani, C.; Dominguez, A. Titanium as a Biomaterial for Implants. In Recent Advances in Arthroplasty; Fokter, S., Ed.; InTech: Rijeka, Croatia, 2012; pp. 149–162.

Rawaa Abbas Mohammed*, Dunya Edan AL-Mammar: Using natural materials as corrosion inhibitors for carbon-steel on phosphoric acid medium. Iraqi Journal of Science, 2019, Special Issue,pp: 40-45. https://doi: 10.24996/ijs.2019.S.I.7

Seung Yeong Cho, Gwang Yong Shin, Do Sik Shim. Effect of laser remelting on the surface characteristics of 316L stainless steel fabricated via directed energy deposition. Journal of Materials Research and Technology. Volume 15, November–December 2021, Pages 5814-5832.

Standard, A. 2009. G61-86. Standard test method for conducting cyclic potentiodynamic polarization measurements for localized corrosion susceptibility of iron-, nickel-, or cobalt-based alloys, ASTM standards. Philadelphia, PA: ASTM.

Standard, A. 2015. F2129–15. Standard test method for conducting cyclic potentiodynamic polarization measurements to determine the corrosion susceptibility of small implant devices. West Conshohocken, PA: ASTM International.

Standard, A. 2017. F2129–17: Standard test method for conducting cyclic potentiodynamic polarization measurements to determine the corrosion susceptibility of small implant devices. ASTM International, West Conshohocken, PA, 1-9.

Steven Y. Yu,a,*,c John R. Scully,a,*,z and Carrisima M. Vitus: Influence of Niobium and Zirconium Alloying Additions on the Anodic Dissolution Behavior of Activated Titanium in HCl Solutions. Journal of The Electrochemical Society, 148 ~2! B68-B78 ~2001.

Sumanta Mukherjee, Santanu Dhara & Partha Saha (2017): Laser surface remelting of Ti and its alloys for improving surface biocompatibility of orthopaedic implants, Materials Technology. https://doi: 10.1080/10667857.2017.1390931

Wei K, Lv M, Zeng X, Xiao Z, Huang G, Liu M, et al. Effect of laser remelting on deposition quality, residual stress, microstructure, and mechanical

property of selective laser melting processed Ti-5Al-2.5Sn alloy. Mater Char 2019; 150:67e77. https://doi.org/10.1016/j.matchar.2019.02.010

Yasa E, Kruth JP. Microstructural investigation of selective laser melting 316L stainless steel parts exposed to laser remelting. Procedia Eng. 2011; 19:389e95. https://doi.org/10.1016/j.proeng.2011.11.130

Yu Z, Zheng Y, Chen J, Wu C, Xu J, Lu H, et al. Effect of laser remelting processing on microstructure and mechanical properties of 17-4 PH stainless steel during laser direct metal deposition. J Mater Process Technol 2020; 284:116738. https://doi.org/10.1016/j.jmatprotec.2020.116738